J Fluoresc (2016) 26:2311–2320
DOI 10.1007/s10895-016-1927-8

ORIGINAL ARTICLE

Polyoxy-Derivatized Perylenediimide as Selective Fluorescent Ag (I) Chemosensor

Merve Zeyrek Ongun[1] · **Kadriye Ertekin**[2] · **Said Nadeem**[3,4] · **Ozgül Birel**[3]

Received: 19 July 2016 / Accepted: 26 August 2016 / Published online: 13 September 2016

Abstract Recent investigations indicated that same concentrations of the ionic silver have harmful effects on aquatic life, bacteria and human cells. Herein we report chemosensory properties of *N,N′-Bis(4-{2-[2-(2-methoxyethoxy)ethoxy] ethoxy}phenyl) -3,4:9,10-perylene tetracarboxydiimide* (PERKAT) towards ionic silver. The dye doped sensing agents were prepared utilizing ethyl cellulose (EC) and poly (methylmethacrylate) (PMMA) and then forwarded to electrospinning to prepare sensing fibers or mats. The PERKAT exhibited bright emission in embedded forms in EC or in the solvents of N,N-Dimethylformamide (DMF), Dichloromethane (DCM), Tetrahydrofurane (THF) and in the mixture of DCM/ethanol. The PERKAT exhibited selective and linear response for ionic silver in the concentration range of 10^{-10} – 10^{-5} M Ag (I) at pH 5.5. Detection limits were found to be 2.6×10^{-10} and 4.3×10^{-11} M, in solution phase studies and PERKAT doped sensing films, respectively. Cross sensitivity of the PERKAT towards pH and some metal ions was also studied. There were no response for the Li^+, Na^+, K^+, Ca^{2+}, Ba^{2+}, Mg^{2+}, NH_4^+, Ni^{2+}, Co^{2+}, Cu^{2+},Pb^{2+}, Al^{3+}, Cr^{3+},Mn^{2+}, Sn^{2+}, Hg^+, Hg^{2+}, Fe^{2+} and Fe^{3+} in buffered solutions. To the best of our knowledge, this is the first study investigating silver sensing abilities of the PERKAT.

Keywords Polyoxy perylenediimide · Electrospinning · Ag (I) · Fluorescence · Sensor

Introduction

Contamination of the fresh waters with ionic silver has become a matter of concern due to the increasing use of silver in industry medicine and technology. Different forms of silver are found in functional products for water purification, biofilms, dental treatment water, wound healing bandages, pool water, integrated into textile for medicinal benefits, in washing machines and refrigerators and numerous others. This intensive interest towards silver arises from its antibacterial efficiency. Today exposure to silver compounds is widespread owing to the intensive use of soluble silver formulations. On the other hand the Environmental Protection Agency (EPA) limits concentrations of the Ag(I) lower than 1.6 nM for aquatic life and microorganisms, and to 0.9 mM in drinking water [1]. Consequently, analysis of trace amounts of ionic silver is very important. Atomic absorption spectrometry, inductively coupled plasma-atomic emission spectrometry, voltammetry potentiometric applications and spectrofluorimetry have been utilized for detection of Ag(I) in a variety of moieties including biological and environmental samples. Among them fluorescence-based detection methods generally possess advantages of selectivity, sensitivity, and simplicity as compared to the other analytical techniques. The fluorescent based sensing approaches utilize fluorescent dyes and ionophores or their integrated form, fluoroionophores. Up to now a number of fluorescent chemosensors for silver ion have been designed

✉ Kadriye Ertekin
kadriye.ertekin@deu.edu.tr

[1] Chemistry Technology Program, Izmir Vocational School, University of Dokuz Eylul, 35160 Izmir, Turkey

[2] Faculty of Sciences, Department of Chemistry, University of Dokuz Eylul, 35160 Izmir, Turkey

[3] Faculty of Sciences, Department of Chemistry, Mugla Sıtkı Koçman University, Kötekli, 48121 Mugla, Turkey

[4] Department of Medicinal and Aromatic Plants, Köyceyiz Vocational School, Mugla Sıtkı Koçman University, Koyceyiz, 48000 Muğla, Turkey

and tested successfully [2–9]. Most of these studies have been performed in the solution phase. Obviously, studies performed in liquid phase provided valuable information for researchers. Nevertheless, the integration of sensing ionophores with solid state components is necessary for better detection limits. Previous studies on the determination of Ag + ions are compared in detail in Table 1 in terms of the sensing material, analysis media, working range, detection limit, and selectivity. According to the numbers, studies performed in solid state present better detection limits (7, 10–13).

Here we have successfully combined the solid state materials with optical sensing technology for silver detection at sub-nanomolar levels utilizing the electrospun fiber materials. In this study, matrix materials of poly (methyl methacrylate) (PMMA) and ethyl cellulose (EC) were used to produce silver sensing mats. The fluorescent probe: N,N′-Bis(4-{2-[2-(2-methoxyethoxy)ethoxy]ethoxy}phenyl)-3,4:9,10-perylene tetracarboxydiimide (PERKAT) was chosen as the indicator due to the strong absorbance, bright luminescence, large Stoke's shift and excellent photostability.

The electrospun fibers were characterized using scanning electron microscopy (SEM) and their average diameters were evaluated. To our knowledge this is the first attempt using the PERKAT as the fluoroionophore-along with electrospinning approach for silver sensing at sub-nanomolar levels.

Silver Sensing Ionophore and Used Chemicals

Synthesis of N,N′-Bis(4-{2-[2-(2-Methoxyethoxy)Ethoxy] Ethoxy}Phenyl)-3,4:9,10-Perylene Tetracarboxydiimide (PERKAT)

PERKAT was synthesized in our labs according to the reported procedure [13, 14]. Perylene diimide utilized here bears polyoxyethylene substituent groups. Polyoxyethylene chains enhance solubility of the molecule and improve compatibility of the dye with non-ionic polymeric matrices. A short summary of the followed synthetic procedure is given here [14] Perylene-3,4:9,10-tetracarboxylic dianhydride (0.69 mmol), 1 3,4-di{2-[2-(2 methoxyethoxy) ethoxy] ethoxy}aniline (5 mmol) and imidazole (5 g) were heated at 140 °C for 4.5 h under Ar atmosphere. Then HCl (200 mL 2 N) was added into the reaction solution and the resulting mixture was stirred for 1 h at room temperature. Then extracted with $CHCl_3$. The organic phase evaporated under vacuum and crude product was purified by column chromatography. The schematic structure of the employed fluoroionophore is shown in Fig. 1.

(CH_2Cl_2: MeOH, 10:1). FT–IR (cm^{-1}): 2922, 2867, 1704 and 1663 (imide group), 1595, 1512, 1455, 1404, 1361, 1299,1255, 1178, 1124. 1H NMR ($CDCl_3$; δ, ppm): 8.68–8.59 (q, 8H, ArH (perylene)), 7.20–7.02 (6H, ArH),4.15 (8H, $ArOCH_2$–), 3.84 (8H, $ArOCH_2CH_2$–), 3.7 (8H, $-OCH_2$–CH_2OCH_3), 3.63–3.61 (16H, $-OCH_2CH_2O$–), 3.5 (8H, $-CH_2OCH_3$), 3.33 (12H, $-OCH_3$), $C_{64}H_{74}N_2O_{20}$.

The polymers of ethyl cellulose (with an ethoxy content of 46 %) and poly (methyl methacrylate) were purchased from Acros and Aldrich companies, respectively. The plasticizer, dioctyl phthalate (DOP) was supplied from Aldrich. The ionic liquid, 1-butyl-3-methylimidazolium tetrafluoroborate ($BMIMBF_4$) and potassium tetrakis-(4-chlorophenyl) borate were supplied from Fluka. All of the solvents and other chemicals (AAS standards or nitrate salts of the Li^+, Na^+, K^+, Ca^{2+}, Ba^{2+}, Mg^{2+}, NH_4^+, Ni^{2+}, Co^{2+}, Cu^{2+}, Pb^{2+}, Al^{3+}, Cr^{3+},Mn^{2+}, Sn^{2+}, Hg^+, Hg^{2+}, Fe^{2+} and Fe^{3+}) were of analytical grade and purchased from Merck, Fluka, and Riedel, respectively. Aqueous solutions were prepared with freshly deionized ultra pure water (specific resistance >18 MΩ cm, pH 5.5) from a Millipore reagent grade water system. $AgNO_3$ was used for the calibration studies.

Preparation of Sensing Composites and Electrospun Nanofibers

In this study, electrospinning was chosen to fabricate the sensing materials. Conditions of the electrospinning were optimized in order to form bead-free PMMA or EC based continuous fibers by varying the concentrations of plasticizer, PMMA or EC and Room Temperature Ionic Liquids (RTILs) in the composites. The sensing composites were prepared by mixing 240 mg of polymer (PMMA or EC), 192 mg of plasticizer (DOP), 48 mg of ionic liquid and 3 mg of PERKAT in 2.0 mL of DCM:EtOH (25:75). IL-free forms were also prepared for comparison. Then, the viscous solution was taken in a plastic syringe and an electric potential of 27 kV was applied between the needle of the syringe and the substrate coated with an aluminum foil. The distance between the needle and the electrode was 10 cm while the diameter of the needle was 0.40 mm. Flow rate of the solution was maintained at 0.5 mL/h programming the syringe pump.

The concentration of RTIL was varied from 0.0 up to 50.0 % *w*/w (0.0, 5.0, 10.0, 20.0, 40.0, and 50.0 w/w), with respect to the content of PMMA or EC. It was found that the presence of the optimum amount of RTILs in the PMMA solutions facilitates the electrospinning of bead-free fibers from the lower polymer concentrations. This behavior can be attributed to the ionic conductivity and proper viscosity of the RTIL doped precursor polymer solutions. Schematic structure of the electrospinning apparatus has been Publisher earlier [9] Fig. 2 reveals SEM images of EC and PMMA based electrospun membranes under various magnifications.

While, the EC based cocktails exhibiting a micro scale porous structure, the PMMA based ones were in fiber forms. In both cases, the empty spaces of the holes within the network structures allow diffusion of ionic silver into the plasticized matrix. It was observed that the electrospun membranes

Table 1 Former studies on the determination of Ag (I)ions in terms of the chemosensor, analysis media, working range, detection limit, and selectivity

Chemosensing agent	Matrix /Response	Working range	LOD	Stability/Reversibility selectivity	Ref No
Boradiazaindacenes, Ratiometric chemosensor with large pseudo-Stokes' shift ((λex), 480 nm)	THF	Ag + (0–10 μM)	-	No interference for $Pb^{2+,}$ Mn^{2+}, Fe^{2+}, Hg^{2+}, and Co^{2+}	[2]
Peripherally functionalized zinc-phthalocyanine bearing benzofuran derivative (λex 345 nm, 616 nm.	THF / Quenching in emission intensity	1.0–50 μM Ag^{+}	-	-	[3]
Rosamine based fluorescent probe , λex = 520 nm.	Ethanol/Enhancement in fluorescence intensity	0.0–5.0 μM Ag+	10^{-7} M Ag+	Selectivity over Cd^{2+}, Cu^{2+}, Hg^{2+}, Na^{+}, Mg^{2+}, Ni^{2+}, Pb^{2+}, Fe^{3+}, and $Zn^{2+)}$	[4]
Bis-pyrene derivative bearing two pyridine groups (λex = 344 nm	Ratiometric response in DMSO-HEPES	0.0–20 μM Ag^{+}	-	Selectivity over Al^{3+}, Ca^{2+}, Cd^{2+}, Co^{2+}, Cu^{2+}, Fe^{2+}, Fe^{3+}, Hg^{2+}, K^{+}, Li^{+}, Mg^{2+}, Mn^{2+}, Na^{+}, Ni^{2+}, Pb^{2+}, Sr^{2+}, and Zn^{2+}	[6]
Two different Zn (II) phthalocyanine derivatives ((λex) 640, (λem) 717 nm)	Plasticized Ethyl cellulose (EC) (Thin Film Form)	10^{-10} -10^{-4} M Ag^{+}	7.6×10^{-12} and 2.3×10^{-11} M	No interference for Li^{+}, Zn^{2+}, Cu^{2+}, Ni^{2+}, Co^{2+}, Hg^{2+}, Pd^{2+}, Sb^{3+}, Al^{3+}, Bi^{3+} Stabel At least 180 days	[7]
Bis-triazolocoumarins on sugar templates ((λex) 345, (λem) 400–550 nm	Salty water Fluorescence quenching	Ag^{+} (0–10 μM)	-	High sensitivity, no cross sensitivtiy towards (Na^{+}, K^{+}, Mg^{2+}, Ca^{2+}, Cu^{2+}, Co^{2+}, Cd^{2+}, Mn^{2+}, Ni^{2+},Zn^{2+})	[8]
Azacrown[N,S,O] into furoquinoline fluorophore (λex) 380 nm) λem 519 nm, ratiometic response	Ethanol	-	-	High sensitivtiy for Ag^{+}, No cross sent. For (Cr^{3+}, Fe^{3+}, Cu^{2+}, Hg^{2+}, Zn^{2+}, Cd^{2+}, and $Pb^{2+,}$, slight sensitivty for Ca^{2+}, Mg^{2+}, Co^{2+}, Ni^{2+}, K^{+}, and Mn^{2+}	[6]
(1,2-bis(4-methoxybenzylidene) hydrazine)	poly(methyl methacrylate) PMMA, EC and ionic liquid, 1-ethyl-3-methylimidazolium tetrafluoroborate (Electrospun nano fiber)	10^{-12} -10^{-6} M Ag^{+}		No interference for Li^{+}, Na^{+}, K^{+}, Ca^{2+}, Ba^{2+}, Mg^{2+}, NH_4^{+}, Ni^{2+}, Co^{2+}, Cu^{2+}, Pb^{2+}, Al^{3+}, Cr^{3+},Mn^{2+}, Sn^{2+}, Hg^{+}, Hg^{2+}, Fe^{2+} and Fe^{3+} No selectivity for F^{-}, Cl^{-}, Br^{-}, $NO3^{-}$, NO_2^{-},SO_4^{2-} and PO_4^{3-}	[9]
Fluorescently labeled single-stranded DNA (ssDNA) probe that adsorbs on nano-C60,	10 mM 3-(N-morpholino)propanesulfonic acid (MOPS) buffer containing 50 mM $NaNO_3$ (pH 7.0).	0–400 nM Ag^{+}	1 nM Ag^{+}	Selectivity over Ca^{2+}, Cd^{2+}, Co^{2+}, Cu^{2+}, Fe^{2+}, Fe^{3+}, Mg^{2+}, $Mn^{2+,}$ Ni^{2+}, Pb^{2+}, and Zn^{2+},	[10]
Graphene oxide exonuclease III-assisted signal amplification. In the presence of Ag(I), the self-hybridization of cytosine-rich ss-DNA labeled with the fluorescent tag FAM	−/Strong amplification of fluorescence.	1–250 nM	0.1 nM	Selectivity over Fe^{3+}, Zn^{2+}, Cu^{2+}, Hg^{2+}, Co^{2+}, Cd^{2+}	[11]
Ion-imprinted fluorescent on–off sensor/ monomer (E)-3_,6_-bis (allyloxy)-2-((thiazol-2-ylmethylene)amino)-4a_, 9a_-dihydrospiro[isoindoline-1,9_-xanthen]-3-one	Detection at 490 nm /phosphate buffer pH 7.4	10 to 60 μM	-	Selectivity over Al^{3+}, Ba^{2+}, Ca^{2+},Co^{2+}, Cu^{2+}, Fe^{2+}, Hg^{2+}, Ni^{2+}, Pb^{2+}, Zn^{2+}	[12]
Polyoxy-derivatized Perylenediimide in DCM-EtOH and in the polymers of ethyl cellulose and poly(methyl methacrylate)	Fluorescence quenching, Detection at 490 nm /in DCM-EtOH Detection at 390 nm in solid state Sensor calibrated with Ag (I) containing acetate buffer at pH 5.5	10^{-9}–10^{-3} M [Ag+] in DCM-EtOH and 10^{-10}–10^{-5} M Ag + in solid state	2.6×10^{-10} and 4.3×10^{-11} M [Ag+] for solution and solid state, respectively	Selectivity over 10^{-3} M of Li^{+}, Na^{+}, K^{+}, Ca^{2+}, Ba^{2+}, Mg^{2+}, NH_4^{+}, Ni^{2+}, Co^{2+}, Cu^{2+},Pb^{2+}, Al^{3+}, Cr^{3+},Mn^{2+}, Sn^{2+}, Hg^{+}, Hg^{2+}, Fe^{2+} and Fe^{3+} ions	This work

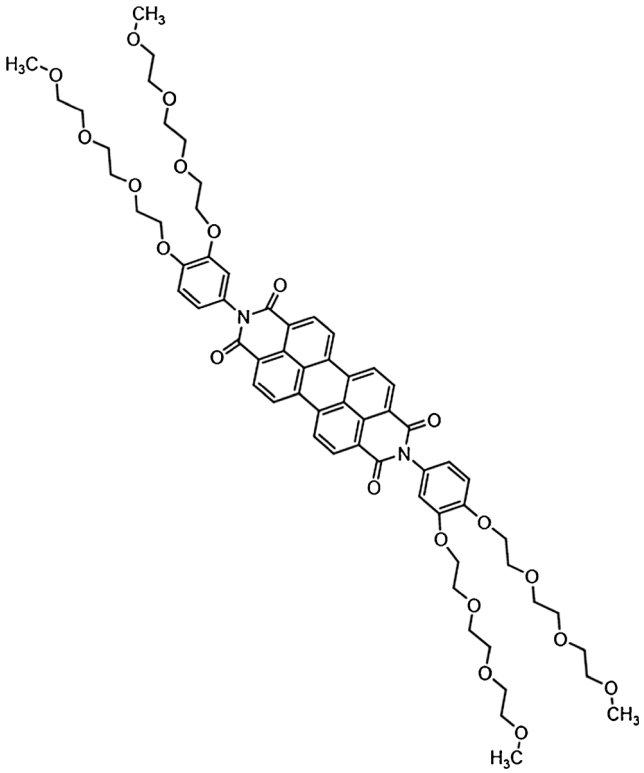

Fig. 1 Structure of the ***N,N′-Bis(4-{2-[2-(2-methoxyethoxy)ethoxy]ethoxy}phenyl)-3,4:9,10-perylene tetracarboxydiimide*** **(PERKAT)**

made up of PMMA exhibited 3D network like structure with a random fiber orientation that was evenly distributed on the substrate. The diameters of the fibers varied between 1.2 μm and 146 nm (See Fig. 2). This type of fibrous-structure of the electrospun membrane provided higher surface area than that of the conventional continuous thin films. Further increase of the surface area may be achieved by changing the conditions of the electrospinning process such as solvent composition, viscosity, concentration, temperature, humidity and working distance, which results in either smaller diameter fibers or increased porosity at the fiber surface.

Apparatus

UV-vis spectra were recorded by using a Shimadzu 2101 UV-visible spectrophotometer. Emission spectra were recorded using a Varian Cary Eclipse or FLS920 instrument from Edinburg Instruments. Lifetime measurements were recorded by a Time Correlated Single Photon Counting TCSPC) system (Edinburgh Instruments (UK). The instrument was equipped with a Standard15W Xe lamp and laser or a microsecond flash lamp for steady- state and lifetime measurements, respectively. During measurements, the Instrument Response Function (IRF) was obtained from a non-fluorescing suspension of a colloidal silica (LUDOX30%, Sigma Aldrich) in water, held in 10 mm path length quartz cell and was considered to be wavelength independent. All lifetimes were fit to a $\chi 2$ value of less than1.1and with residuals trace symmetrically distributed around the zero axes. All of the measurements were performed at room temperature.

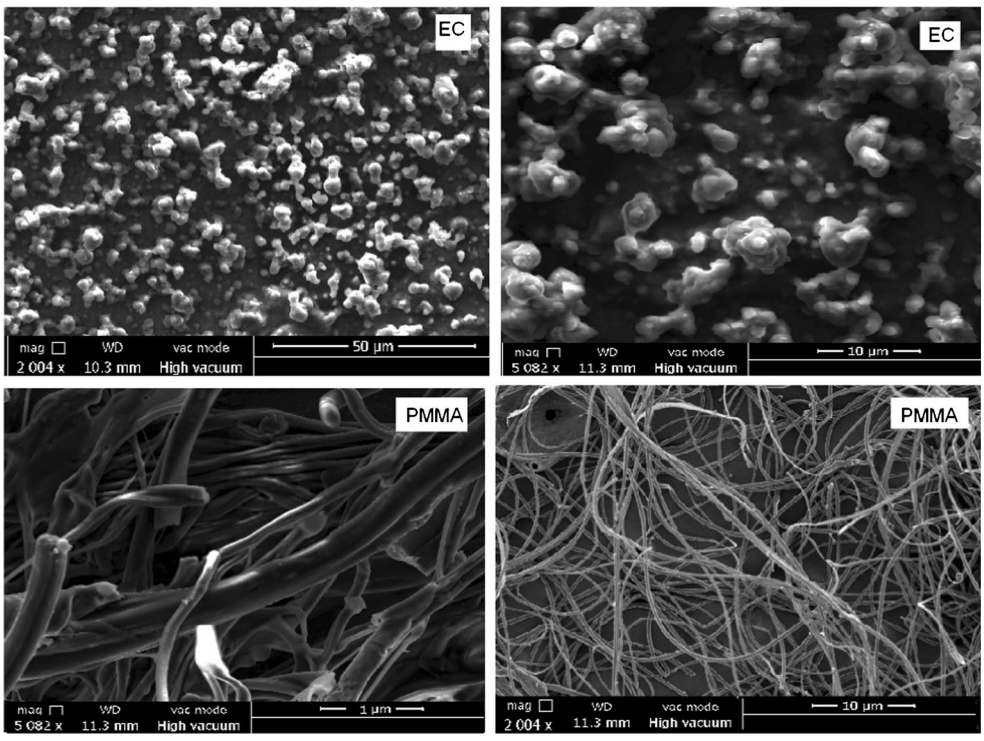

Fig. 2 SEM images of EC and PMMA based electrospun membranes under various magnifications

Spectral Characterization of the Fluoroionophore

Absorption, excitation and emission spectra of the PERKAT were recorded in the solvents of DMF, DCM, THF, and in mixture of toluene/ethanol 80:20 (*v*/v), respectively. In all of the solvents the dye exhibited two distinct absorption maxima with high molar extinction coefficients, around 490 and 526 nm, respectively (See Fig. 3). The dye exhibited highest absorption efficiency in DMF. Absorption maxima observed in the visible side of the spectrum located between 487 and 530 nm corresponds to $\pi - \pi^*$ singlet transitions reported for the perylenediimide.

Spectral data of the dye were shown in Table 2. Upon excitation around 485 nm, the dye displayed emission maxima at 532, 532, 525, and 539 nm in the solvents of DMF, DCM, THF and DCM:EtOH, respectively. As can be seen from Table 2, the dye can be excited around 485 nm or further wavelengths in the solvents. However when encapsulated in polymeric matrices the excitation maximum shifts to shorter wavelengths, 340 or 349 nm for EC and PMMA, respectively. The highest and lowest Stoke's shift values of 50 and 36 nm were observed in EC and in PMMA, respectively. Due to the higher Stoke's shift, the EC matrix was chosen for further sensing studies.

Cross Sensitivity towards Acidic or Alkaline Species

In most cases the calibration standards are either in acidic form or should be acidified to prevent the precipitation of the ion under investigation. Therefore, cross sensitivity of the chromoionophore towards pH should be questioned.

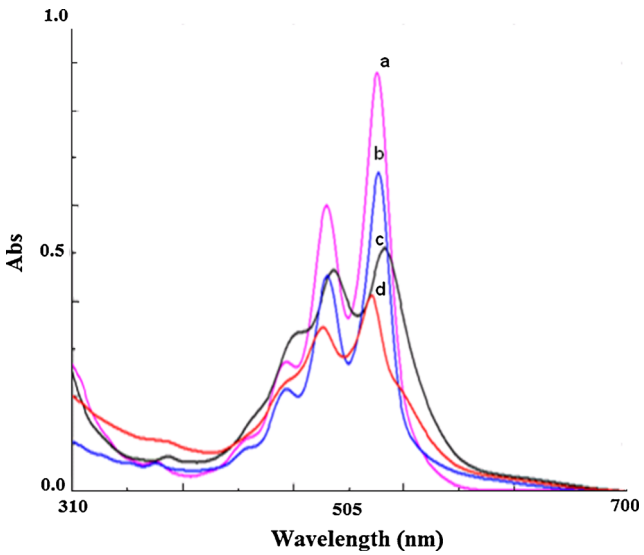

Fig. 3 Absorption spectra of the PERKAT in different solvents a) DMF b) DCM c) DCM:EtOH (20:80) d) THF

We investigated effect of the acidic and alkaline species on emission performance of PERKAT. We spectrofluorimetrically titrated 10^{-5} M solution of the PERKAT (in DCM) with non-aqueous $HClO_4$ (10^{-3} M in dioxane) and strong quaternary ammonium base; tetrabutylammonium hydoxide (10^{-3} M in 2-propanol). We recorded a high sensitivity both in the acidic and basic regions during titrations. However when encapsulated in EC matrix along with ionic liquid $BMIMBF_4$, the acid-base sensitivity of the PERKAT diminished significantly. Figure 4 I and II reveals acid-base response of the EC encapsulated PERKAT towards strong acids and bases, respectively.

Even in encapsulated forms; the dye is still sensitive to strong acidity around pH 1.0. However at higher pH values of 3.0, this effect is not significant and can be overcome utilizing the calibration standards in the buffered solutions. The encapsulated forms of the PERKAT along with the ionic liquid exhibited both short and long term stability with respect to the IL-free forms. The tuned sensitivity and long term stability of the PERKAT in EC can be attributed to the intrinsic buffering effect of the ionic liquid. The $BMIMBF_4$ acts like a buffer system by neutralizing the acidic species due to the formation of weak Lewis acid–base complexes between proton and anionic side of the RTIL. Formation of such a buffer-like system tunes the sensitivity of the sensor and enhances the long-term stability of the indicator since it slowly acts as a sink for acidic species in the ambient air. Similar effects of the RTILs have been observed in our previous studies [15, 16].

For further metal ion sensing studies we employed buffered solutions keeping the acidity constant at pH 5.5. The effect of pH on the complexation of PERKAT with Ag (I) ions was investigated between pH 2.5 and 7.0 at fixed metal ion concentration of 10^{-5} mol L^{-1}. The relative signal change; $(I_0 - I)/I_0$ produced by the Ag (I) ions was high and stable around pH 5.5. Distribution of the chemical species in the working conditions was theoretically checked with chemical equilibrium software programme (Visual MINTEQ). At pH 5.5 abundance of the acetate (CH_3COO^-(aq)) acetic acid CH_3COOH(aq) and Ag^+(aq) were 36.4 %, 66.6 % and 100.0 %, respectively. Due to the excellent solubility of silver, the acetic acid/acetate buffered solutions of pH 5.5 were chosen as working moiety further studies.

Silver Uptake into the Mats and Fluorescence Based Response

When doped into the EC matrices along with the anionic additive, potassium tetrakis-(4-chlorophenyl) borate, the PERKAT dye becomes a Ag (I) selective probe. In this system, silver ions are selectively extracted into the porous films (mats) by the anionic additive meanwhile potassium ions diffuse from the membrane into the aqueous phase due to the

Table 2 Absorption and emission based spectral data of the dye acquired in different moieties

Matrix	λ^1_{abs}	λ^2_{abs}	ε_{max} (λ^1_{abs})	ε_{max} (λ^2_{abs})	(Excitation wavelength) λ_{max}^{ex}	(Emission wavelength) λ_{max}^{em}	Stoke's shift $\Delta\lambda$(nm)
DMF	490	526	12,060	17,560	485	535	50
DCM	490	526	9120	13,400	485	532	47
THF	487	521	8240	6900	478	525	47
DCM:EtOH	495	530	9340	10,200	491	539	48
EC					340	390	50
PMMA					349	385	36

mechanism of ion-exchange. Physical aspect of the response mechanism of PERKAT dye can be explained by the following ion-exchange pathway shown in Eq. (1).

$$\begin{aligned} &PERKAT_{(org)\ (pink)} + 2K^+_{(org)} + 2TpCIPB^-_{(org)} \\ &\quad + 2Ag^+(aq) \leftrightarrow PERKATAg_2{}^+_{(org)\ (colorless)} \\ &\quad + 2TpCIPB^-_{(org)} + 2K^+_{(aq)} \end{aligned} \quad (1)$$

Figures 5 and 6 show the change in fluorescence spectra of solution and electrospun materials as a function of different concentrations of silver ions. Upon exposure to Ag (I) ions, both the solution and EC based electrospun materials exhibited similar fluorescence signal change in direction of fluorescence quenching. Signal drops observed at the emission maxima of 534 nm or 572 nm can be followed as the analytical signal for the concentration range of 10^{-9}–10^{-3} M in solution phase. In EC

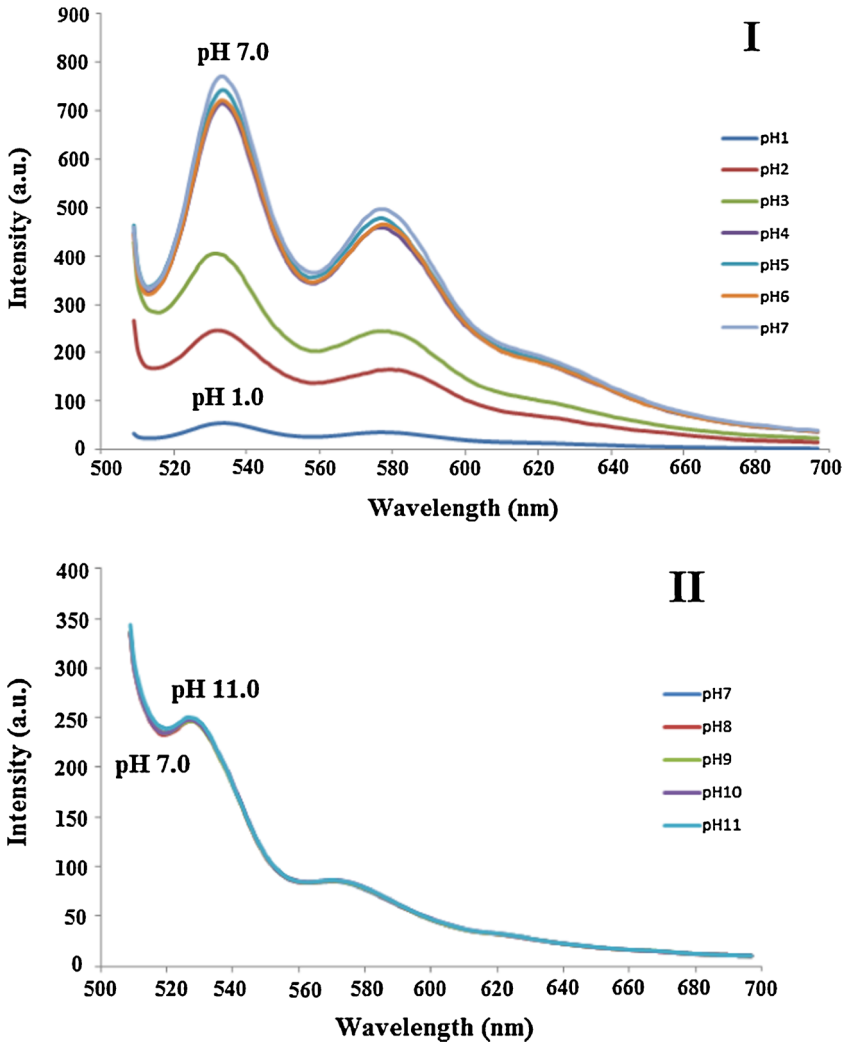

Fig. 4 I: Acid base sensitivity of PERKAT encapsulated in EC in the pH range of 1.0–7.0. II: pH range of 7.0–11.0. Buffer solutions were prepared with 0.01 M CH_3COOH, 0.01 NaOH, 0.01 M NaH_2PO_4, and 0.01 M BES at desired pH

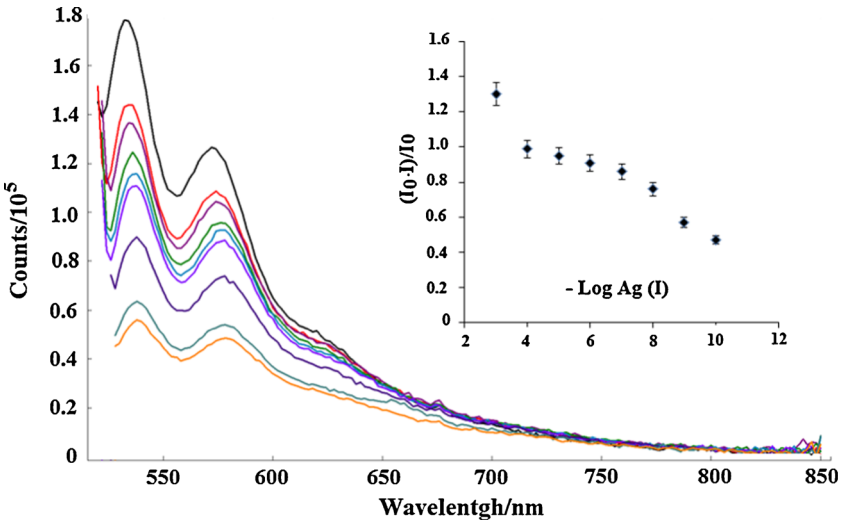

Fig. 5 Fluorescence response of the (a) Ag-free solution in DCM-EtOH, (b) 10^{-9} M, (c) 10^{-8} M, (d) 10^{-7} M, (e) 10^{-6} M, (f) 10^{-5} M, (g) 10^{-4} M, (h) 10^{-3} M Ag (I). Inset: calibration plot for the concentration range of 10^{-9} to 10^{-3} M Ag (I)

based forms the signal quenching at 390 nm is very stable and repeatable. The working range shifted to lower concentrations, and exhibited a more liner response between10^{-10} -10^{-5} M Ag(I) when the dye was embedded in the EC (See Figs. 5 and 6). The calibration curves were plotted by taking the mean values of four different solutions (n = 4) of the same medium.

Detection limits in solution and PERKAT doped sensing films were found to be 2.6 × 10^{-10} and 4.3 × 10^{-11} M, respectively (The LOD values have been calculated utilizing concentration of the metal ion giving a signal equal to average of the blank signal (for n = 20) plus three standard deviations). The data given in Table 1 indicate that, the LOD associated with the proposed sensing material for Ag(I) ion is undoubtedly superior with respect to that of most of other silver probes. The intensity decrease is known to be due to the quenching of the PERKAT by Ag (I) ions. In many instances the fluorophore can be quenched both by collisions and by complex formation. The intensity based data (I_0/I) or (I_0 − I)/I_0 exhibiting an upward-concave curvature towards the y-axis is the evidence of combined quenching both by collisions (dynamic quenching) and by complex formation (static quenching) with the same quencher [17]. In case of dynamic quenching the collisions between the quencher and the fluorophore affect only the excited state of the fluorophore, no changes in the absorption or excitation spectrum are expected. On the contrary, the formation of ground-state complex in static quenching will perturb the absorption spectra of the fluorophore.

Thus, a careful examination of the absorption spectrum would be helpful to distinguish static and dynamic quenching. Figure 7 depicts the absorption spectrum of PERKAT dye in the absence and presence of Ag (I) ions (See spectrum "a" and "b"). Dramatic changes observed in the absorption integral upon exposure to ionic silver reveal formation of a non-fluorescent complex with Ag (I) in the ground state. When the linear shape of the fluorescence intensity based response data were evaluated together, the quenching mechanism between PERKAT and Ag (I) can be concluded as "static" quenching. Measurement of fluorescence lifetimes also

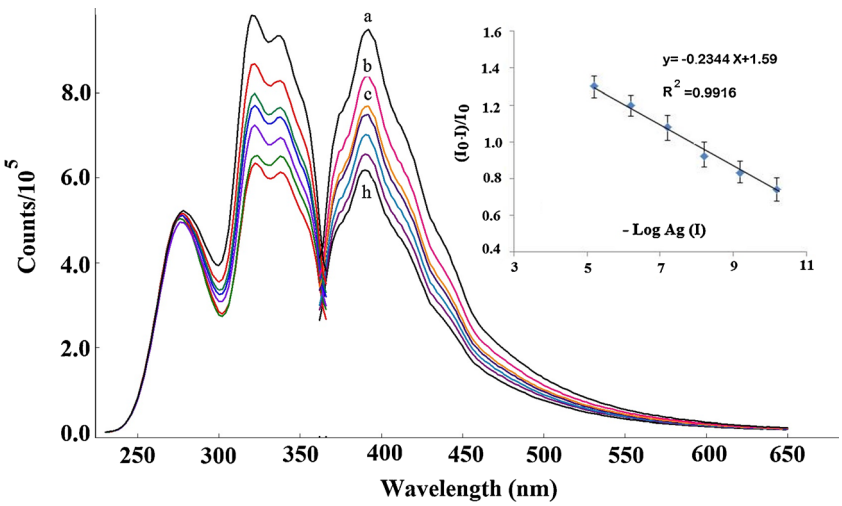

Fig. 6 Excitation–emission based response of the dye-doped EC based electrospun mats to Ag (I) ions at pH 5.5. (a) Ag-free buffer, (b) 10^{-10} M, (c) 10^{-9} M, (d) 10^{-8} M, (e) 10^{-7} M, (f) 10^{-6} M, (g) 10^{-5} M Ag (I). Inset: calibration plot for the concentration range of 10–10 to 10–5 M Ag (I)

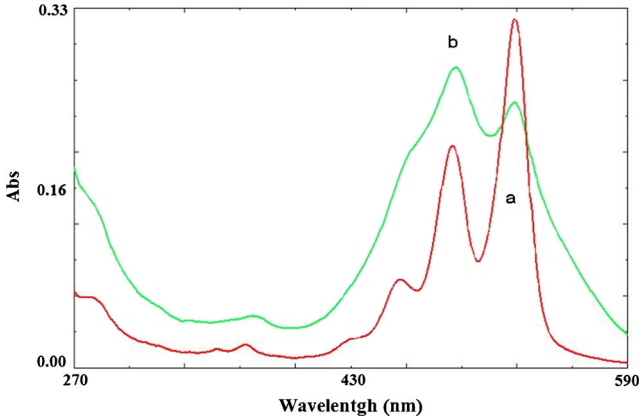

Fig. 7 Absorption spectra of the PERKAT in DCM: EtOH (20:80) a: Ag(I) free b: Ag (I) containing moieties

supported our findings. Figure 8 compares decay curves of the Ag (I)-free and Ag (I) containing solutions of the PERKAT. Bi-exponential decay times of 2.15 ± 0.1 (7.2 %) and 13.4 ± 0.1 (92.8 %) nanoseconds were measured for the Ag-free forms. The decay times of 2.14 ± 0.1 (7.3 %) and 13.6 ± 0.1 (92.7 %) nanoseconds reported for Ag containing forms can be concluded as the evidence of static quenching.

The method of continuous variation (Job's method) was used to determine the stoichiometry of the binding and a 1:2 complex formation of PERKAT: $2Ag^{+}$ was suggested, consistent with Job's plot analysis (See Fig. 9).

Selectivity

Calcium, magnesium, potassium and sodium, which are the most abundant ions in natural water samples as well as physiologically relevant species and could be potential interferents for determination of the Ag (I). In chemosensing based approaches, affinity of chromoionophores for the above

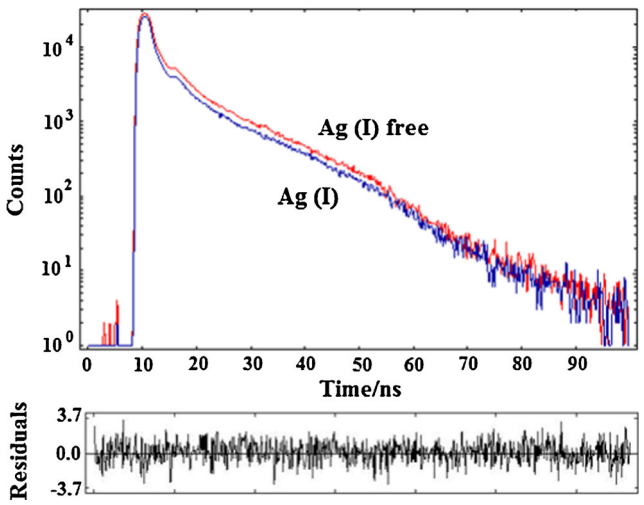

Fig. 8 Decay curves of PERKAT in DCM: EtOH (20:80) in the absence and presence of the ionic silver

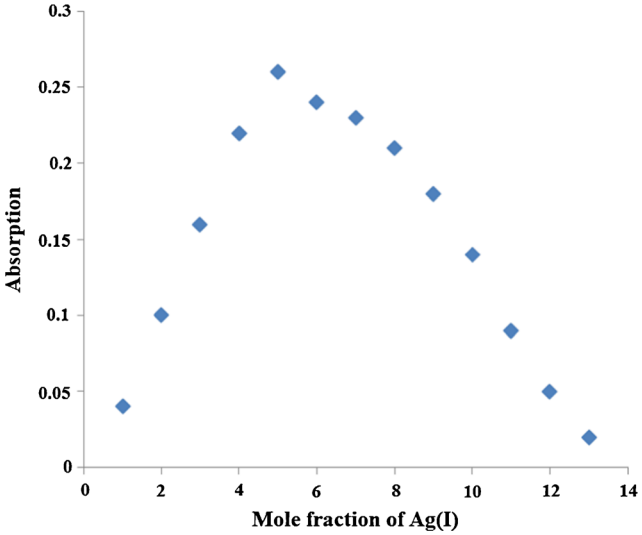

Fig. 9 Job's plot based on the absorption intensity of **PERKAT**-Ag(I) at 486 nm in DCM:EtOH solution (20:80 *v*/v), [PERKAT + Ag(I)] = 100 μmol L^{-1}

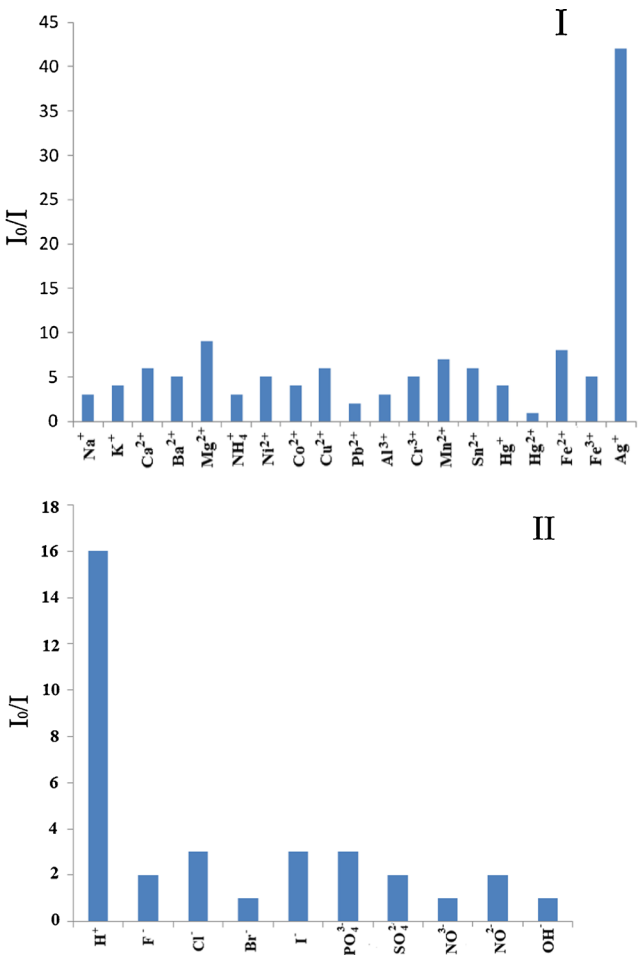

Fig. 10 Response of EC based fibers for the 10^{-3} M concentrations of metal ions at pH 5.5. II: Response of the same composition towards conventional anions and proton

mentioned metal ions is still a problem. In order to reveal the selectivity of the proposed method on ionic silver, the influence of a number of cations were investigated.

Tests were performed in presence of 10^{-3} M of Li^+, Na^+, K^+, Ca^{2+}, Ba^{2+}, Mg^{2+}, NH_4^+, Ni^{2+}, Co^{2+}, Cu^{2+},Pb^{2+}, Al^{3+}, Cr^{3+},Mn^{2+}, Sn^{2+}, Hg^+, Hg^{2+}, Fe^{2+} and Fe^{3+} ions in acetic acid/acetate buffered separete solutions at pH 5.5. From Fig. 10-I, it can be concluded that, the sensing membranes are capable of determining Ag (I) with a high selectivity over other ions. The fluorescence was dramatically quenched in the presence of Ag + at 390 nm exhibiting an I_0/I ratio of 41. The interference effects of the anions of F^-, Cl^-, Br^-, NO_3^-, NO_2^-, SO_4^{2-} PO_4^{3-} and proton were also tested. The sensing agents exhibited negligible signal changes when exposed to all of the conventional anions at pH 5.5 (See Fig. 10-II). Only very high concentrations of proton caused a considerable signal change which can be overcome using buffered solutions under test conditions.

Response Time, Regeneration and Stability

The sensor exhibited a very fast but non-reversible response towards 10^{-4} M of Ag (I) in solution phase studies. The response time (τ_{90}) was less than 30 s. However, in solid state the response was fully reversible and only a slight drift (1.89 %) on the upper signal level has been observed after 15 cycles. Response and regeneration experiments were carried out utilizing 10^{-4} M Ag (I) containing CH_3COOH/CH_3COO^-buffer (10^{-3} M) and slightly acidic 0.1 M EDTA solutions, alternatively. Approximately100% regeneration performance was succeeded with 0.1 M thiourea. However due to the toxicity considerations, for further regeneration treatments 0.01 M CH_3COOH/CH_3COO^- buffered EDTA solutions (at pH: 4.5) were preferred. The average response and regeneration times for EC based structures were measured as 3.5 and 7.5 min ($n = 15$). Between the 1st and 15th cycles, the level of reproducibility achieved was quite good and exhibited a SD of 309.5 ± 6.7 and RSD% 2.2 for upper signal level, respectively (see Fig. 11). Figure 11 also reveals short term stability of the encapsulated forms of PERKAT. We have demonstrated that the $BIMIMBF_4$ doped sensor fibers and mesoprorous slides exhibited a stable and reproducible response for silver measurements for a large concentration range. The sensing composites were left in the lab atmosphere in a dessicator and long term stabilities were tested within certain time intervals, during 8 months. There was no significant signal drift or instability in their response to oxygen even after 14 months. Our long term stability tests are still in progress.

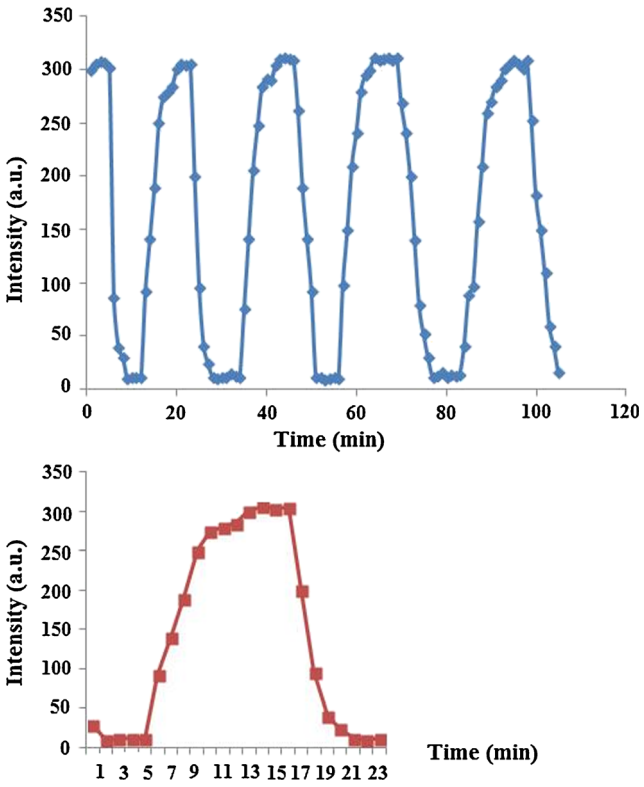

Fig. 11 The response and regeneration dynamics of the EC based structures after exposure to 10^{-4} M of Ag (I) for 5 successive cycles

Conclusion

Herein we report sensing properties of *N,N′-Bis(4-{2-[2-(2-methoxyethoxy)ethoxy] eth- oxy}phenyl) -3,4:9,10-perylene tetracarboxydiimide* (PERKAT) towards ionic silver as well as other potential interferants. In this work, we performed coupling of polymeric electrospun materials with fluorescence-based measurement technique without scattering and other side effects. We performed to measure the Ag (I) concentrations as low as 10^{-11} M exploiting the dye along with solid state materials. Our sensing approach resulted with large linear working ranges extending to 10^{-11}–10^{-5} mol L^{-1} Ag (I). Utilization of the ionic liquid within the matrix enhanced the long term stability of the molecule considerably. Further efforts will focus on exploring new sensing materials and polymer compositions, controlling the size of the electrospun membranes, and optimizing the sensitivities for the detection of a variety of analytes.

Acknowledgments Funding this research was provided by Scientific Research Funds of Dokuz Eylul University and the Scientific and Technological Research Council of Turkey (TUBITAK).

References

1. EPA (Environmental Protection Agency) (1980) Ambient water quality criteria for silver. EPA 4405–80-071. Office of Water Regulations, Washington DC
2. Coskun A, Akkaya EU (2005) Ion sensing coupled to resonance energy transfer: a highly selective and sensitive ratiometric fluorescent chemosensor for Ag (I) by a modular approach. J Am Chem Soc 127:10464–10465

3. Kandaz M, Güney O, Senkal FB (2009) Fluorescent chemosensor for Ag (I) based on amplified fluorescence quenching of a new phthalocyanine bearing derivative of benzofuran. Polyhedron 28: 3110–3114
4. Iyoshi S, Taki M, Yamamoto Y (2008) Rosamine-based fluorescent chemosensor for selective detection of silver (I) in an aqueous solution. Inorg Chem 47:3946–3948
5. Shamsipur M, Alizadeh K, Hosseini M, Caltagirone C, Lippolis V (2006) A selective optode membrane for silver ion based on fluorescence quenching of the dansylamidopropyl pendant arm derivative of 1-aza-4,7,10-trithiacyclododecane([12]aneNS3. Sensors Actuators B Chem 113:892–899
6. Wang H, Xue L, Qian Y, Jiang H (2010) Novel ratiometric fluorescent sensor for silver ions. Org Lett 12:292–295
7. Topal SZ, Gürek AG, Ertekin K, Yenigul B, Ahsen V (2010) Fluorescent probes for silver detection employing phthalocyanines in polymer matrices. Sens Lett 8:1–8
8. He XP, Song Z, Wang ZZ, Shi XX, Chen K, Chen GR (2011) Creation of 3,4-bis-triazolocoumarinesugar conjugates via flourogenic dual click chemistry and their quenching specificity with silver(I) in aqueous media. Tetrahedron 67:3343–3347
9. Kacmaz S, Ertekin K, Suslu A, Ozdemir M, Ergun Y, Celik E, Cocen U (2011) Emission based sub-nanomolar silver sensing with electrospun nanofibers. Sensors Actuators B Chem 153:205–213
10. Li H, Zhai J, Sun X (2011) Highly sensitive and selective detection of silver (I) ion using nano-C60 as an effective fluorescent sensing platform. Analyst 136(10):2040–2043
11. Lang M, Li Q, Huang H, Yu F, Chen Q (2016) Highly sensitive exonuclease III-assisted fluorometric determination of silver(I) based on graphene oxide and self-hybridization of cytosine-rich ss-DNA. Microchim Acta 183:1659–1665
12. Sun H, Lai JP, Lin DS, Huang XX, Zuo Y, Lia YL (2016) A novel fluorescent multi-functional monomer for preparation of silver ion-imprinted fluorescent on–off chemosensor. Sensors Actuators B Chem 224:485–491
13. Langhals H, Ismael R, Yuruk O (2000) Persistent fluorescence of perylene dyes by steric inhibition of aggregation. Tetrahedron 56: 5435–5441
14. Birel OH, Zafer C, Dincalp H, Aydin B, Can M (2011) Highly soluble polyoxyethylene-perylene diimide: optical, electrochemical and photovoltaic studies. J Chem Soc Pak 33(4):562–569
15. Oter O, Ertekin K, Derinkuyu S (2008) Ratiometric sensing of CO_2 in ionic liquid modified ethyl cellulose matrix. Talanta 76:557–563
16. Oter O, Ertekin K, Topkaya D, Alp S (2006) Emission-based optical carbon dioxide sensing with HPTS in green chemistry reagents: room-temperature ionic liquids. Anal Bioanal Chem 386:1225–1234
17. Lakowicz JR (2006) Principles of Fluorescence Spectroscopy, 3rd edn. Springer Press, New York